Supporting Information

Near-infrared fluorescent organic porous crystal that responds to solvent vapors †

Tsutomu Ishi-i,[*a] Honoka Tanaka,[a,b] Himiko Koga,[a] Yuuma Tanaka,[a] and Taisuke Matsumoto[c]

Table of Contents

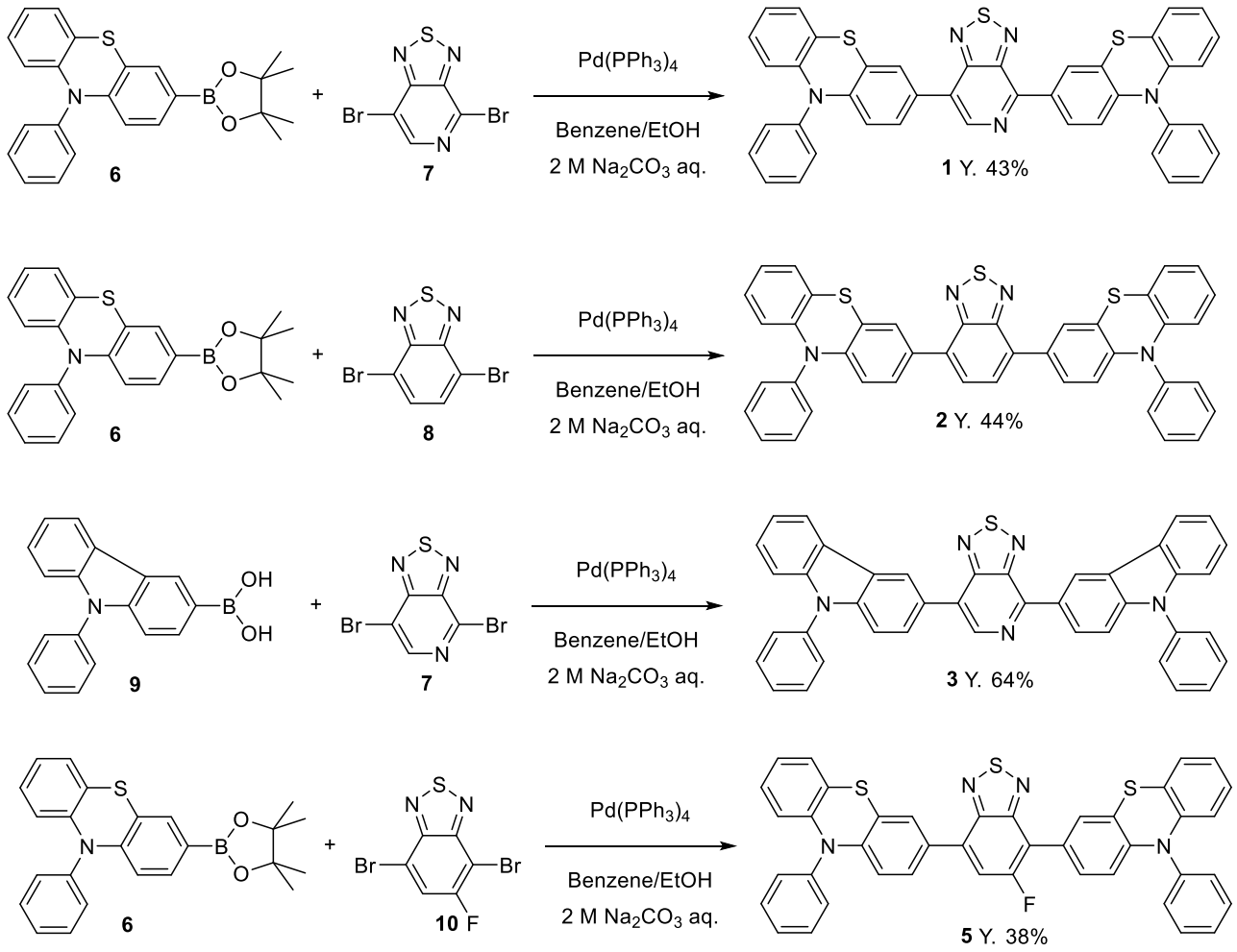

Scheme S1 Preparation of dyes **1**, **2**, **3**, and **5**.

Experimental Section

General. All melting points are uncorrected. IR spectra were recorded on a JASCO FT/IR-470 plus Fourier transform infrared spectrometer, and measured on KBr pellets. ^{1}H and ^{13}C NMR spectra were determined in $CDCl_3$ or CD_2Cl_2 with a JEOL ECX 500 spectrometer. Residual solvent protons were used as internal standard and chemical shifts (δ) are given relative to tetramethylsilane (TMS). The coupling constants (J) are reported in hertz (Hz). Elemental analysis was performed at the Elemental Analytical Center, Kyushu University. Fast atom bombardment mass spectrometry (FAB-MS) spectra were recorded with a JEOL JMS-70 mass spectrometer with m-nitrobenzyl alcohol (NBA) as a matrix. Gel permeation chromatography (GPC) was performed with a Japan Analytical Industry LC-908 using JAIGEL-1H column (20 × 600 mm) and JAIGEL-2H column (20 × 600 mm) eluting with chloroform (3.0 mL/min). Analytical TLC was carried out

on silica gel coated on aluminum foil (Merck 60 F254). Column chromatography was carried out on silica gel (WAKO C300). Preparation of **4** was already reported previously.[1] Compound **6** was prepared according to a method reported previously.[2]

4,7-Bis(N-phenylphenothiazine-3-yl)[1,2,5]thiadiazolo[3,4-c]pyridine (1). To a mixture of boronate **6**[2] (482 mg, 1.2 mmol), dibromide **7** (147 mg, 0.5 mmol), and tetrakis(triphenylphosphine)palladium(0) (81 mg, 0.07 mmol) were added in deaerated benzene (5 mL), ethanol (1.3 mL), and aqueous 2 M sodium carbonate (2.5 mL). Then the mixture was heated at 85 °C under an argon atmosphere for 21 h. After the reaction mixture was poured into water, it was extracted with dichloromethane. The combined organic layer was washed with brine and water, dried over anhydrous magnesium sulfate, and evaporated in vacuo to dryness. The residue was purified by silica gel column chromatography (WAKO C300) eluting with chloroform and by GPC eluting with chloroform to give **1** in 43% (147 mg, 0.215 mmol). An analytical sample was obtained by recrystallization from hexane/chloroform as a dark violet solid: mp 271–273 °C; IR (KBr, cm^{-1}) 3060, 3034, 1589, 1575, 1491, 1467, 1448, 1313, 1259, 1247, 744, 700, 668; ^{1}H NMR ($CDCl_3$, 500 MHz) δ 6.15 (dd, J = 1.7, 8.0 Hz, 1 H, ArH), 6.19 (dd, J = 1.7, 8.0 Hz, 1 H, ArH), 6.28 (d, J = 8.6 Hz, 1 H, ArH), 6.31 (d, J = 8.6 Hz, 1 H, ArH), 6.80–6.88 (m, 4 H, ArH), 7.01–7.06 (m, 2 H, ArH), 7.44 (d, J = 7.5 Hz, 4 H, ArH), 7.49 (dd, J = 2.3, 8.6 Hz, 1 H, ArH), 7.54 (t, J = 7.5 Hz, 2 H, ArH), 7.64 (t, J = 7.5 Hz, 2 H, ArH), 7.65 (t, J = 7.5 Hz, 2 H, ArH), 7.70 (d, J = 2.3 Hz, 1 H, ArH), 8.23 (dd, J = 2.3, 8.6 Hz, 1 H, ArH), 8.36 (d, J = 2.3 Hz, 1 H, ArH), 8.64 (s, 1 H, ArH); ^{13}C NMR ($CDCl_3$, 126 MHz) δ 115.40, 115.91, 115.99, 119.42, 119.52, 119.70, 120.35, 122.72, 122.87, 124.91, 126.67, 126.71, 126.84, 126.93, 127.54, 127.56, 128.57, 128.67, 128.75, 128.95, 130.93, 130.96, 131.03, 140.42, 140.53, 141.58, 143.32, 143.70, 144.57, 145.85, 149.47, 150.02, 156.49; FAB-MS (positive, NBA) m/z 683 (M^+). Anal. Calcd for $C_{41}H_{25}N_5S_3$ (683.87)·0.64$CHCl_3$·0.14C_6H_{14}: C, 66.06; H, 3.60; N, 9.07. Found: C, 66.28; H, 3.44; N, 9.21.

4,7-Bis(N-phenylphenothiazine-3-yl)-2,13-benzothiadiazole (2). According to a method similar to the preparation of **1**, **2** was obtained from boronate **6**[2] (614 mg, 1.53 mmol), dibromide **8** (206 mg, 0.7 mmol), and

tetrakis(triphenylphosphine)palladium(0) (116 mg, 0.10 mmol) were added in deaerated benzene (7 mL), ethanol (1.8 mL), and aqueous 2 M sodium carbonate (3.5 mL). The reaction mixture was purified by silica gel column chromatography (WAKO C300) eluting with hexane/chloroform (6:4, v/v) and by GPC eluting with chloroform to give **2** in 44% (193 mg, 0.307 mmol). An analytical sample was obtained by recrystallization from hexane/chloroform as a red solid; mp 240–241 °C; IR (KBr, cm^{-1}) 3060, 3033, 2924, 2853, 1590, 1490, 1464, 1438, 1306, 1257, 1245, 815, 744, 697; ^{1}H NMR ($CDCl_3$, 500 MHz) δ 6.19 (dd, J = 1.7, 8.0 Hz, 2 H, ArH), 6.30 (d, J = 8.6 Hz, 2 H, ArH), 6.79–6.87 (m, 4 H, ArH), 7.03 (dd, J = 1.7, 8.6 Hz, 2 H, ArH), 7.45 (d, J = 7.5 Hz, 4 H, ArH), 7.49 (dd, J = 2.3, 8.6 Hz, 2 H, ArH), 7.52 (t, J = 7.5 Hz, 2 H, ArH), 7.62 (d, J = 2.3 Hz, 2 H, ArH), 7.63(s, 2 H, ArH), 7.64 (t, J = 7.5 Hz, 4 H, ArH); ^{13}C NMR ($CDCl_3$, 126 MHz) δ 115.84, 116.02, 119.80, 120.28, 122.64, 126.74, 126.85, 126.90, 127.04, 127.80, 128.45, 130.86, 131.06, 131.50, 131.65, 140.91, 143.91, 144.26, 153.98; FAB-MS (positive, NBA) m/z 682 (M^+). Anal. Calcd for $C_{42}H_{26}N_4S_3$ (682.88): C, 73.87; H, 3.84; N, 8.02. Found: C, 73.77; H, 3.92; N, 7.69.

4,7-Bis[N-(phenyl)carbazole-4-yl][1,2,5]thiadiazolo[3,4-c]pyridine (3). According to a method similar to the preparation of **1**, **3** was obtained from boronic acid **9** (189 mg, 0.66 mmol), dibromide **7** (88 mg, 0.3 mmol), and tetrakis(triphenylphosphine)palladium(0) (70 mg, 0.06 mmol) were added in deaerated benzene (6 mL), ethanol (1.5 mL), and aqueous 2 M sodium carbonate (3 mL). The reaction mixture was purified by silica gel column chromatography (WAKO C300) eluting with hexane/chloroform (1:1, v/v) and by GPC eluting with chloroform to give **3** in 64 % (119 mg, 0.192 mmol). An analytical sample was obtained by recrystallization from hexane/dichloromethane as a wine red powder: mp 206–210 °C; IR (KBr, cm^{-1}) 3060, 3041, 1598, 1501, 1446, 1364, 1232, 745, 699; ^{1}H NMR ($CDCl_3$, 500 MHz) δ 7.34–7.40 (m, 2 H, ArH), 7.45–7.47 (m, 4 H, ArH), 7.50–7.55 (m, 2 H, ArH), 7.58–7.69 (m, 10 H, ArH), 8.10 (d, J = 8.6 Hz, 1 H, ArH), 8.28 (d, J = 7.5 Hz, 1 H, ArH), 8.34 (d, J = 7.5 Hz, 1 H, ArH), 8.82 (d, J = 8.6 Hz, 1 H, ArH), 8.84 (s, 1 H, ArH), 9.00 (s, 1 H, ArH) , 9.56 (s, 1 H, ArH); ^{13}C NMR ($CDCl_3$, 126 MHz) δ 109.87, 110.01, 110.06, 110.21, 120.29, 120.51, 120.61, 120.78, 121.22, 122.61, 123.39, 123.81, 123.91, 126.31, 126.35, 126.65, 126.95, 127.21, 127.72, 127.77, 128.02, 129.20, 129.98, 137.33, 137.44, 141.04, 141.40, 141.54, 142.15, 142.61, 152.05, 152.11, 157.29; FAB-

MS (positive, NBA) m/z 619 (M^+). Anal. Calcd for $C_{41}H_{25}N_5S$ (619.74): C, 79.46; H, 4.07; N, 11.30. Found: C, 79.44; H 3.99; N, 11.29.

5-Fluoro-4,7-bis(N-phenylphenothiazine-3-yl)-2,13-benzothiadiazole (5). According to a method similar to the preparation of **1**, **5** was obtained from boronate **6**[2] (260 mg, 0.65 mmol), dibromide **10** (94 mg, 0.3 mmol), and tetrakis(triphenylphosphine)palladium(0) (35 mg, 0.03 mmol) were added in deaerated benzene (6 mL), ethanol (1.5 mL), and aqueous 2 M sodium carbonate (3 mL). The reaction mixture was purified by silica gel column chromatography (WAKO C300) eluting with chloroform and by GPC eluting with chloroform to give **5** in 38 % (79 mg, 0.113 mmol). An analytical sample was obtained by recrystallization from chloroform as a orange solid: mp 329–331 °C; IR (KBr, cm^{-1}) 3062, 3033, 1589, 1576, 1491, 1464, 1439, 1307, 1259, 818, 749, 697, ^{1}H NMR ($CDCl_3$ 500 MHz) δ 6.18 (d, J = 8.6 Hz, 2 H, ArH), 6.29 (d, J = 8.6 Hz, 2 H, ArH), 6.79–6.88 (m, 4 H, ArH), 7.00–7.04 (m, 2 H, ArH), 7.31 (d, J = 8.6 Hz, 1 H, ArH), 7.42–7.55 (m, 9 H, ArH), 7.61-7.67 (m, 5 H, ArH); ^{13}C NMR ($CDCl_3$, 126 MHz) δ 115.46, 115.70, 115.89, 115.96, 118.02, 118.26, 119.40, 119.67, 119.80, 120.26, 122.64, 122.77, 125.29, 126.72, 126.88, 126.97, 127.83, 128.47, 128.50, 128.60, 129.17, 130.19, 130.86, 130.94, 131.05, 131.12, 132.12, 140.54, 140.63, 143.66, 143.87, 144.31, 144.80, 150.88, 155.00, 155.09, 158.38, 160.37; FAB-MS (positive, NBA) m/z 700 (M^+). Anal. Calcd for $C_{42}H_{25}FN_4S_3$ (700.87): C, 71.97; H, 3.60; N, 7.99. Found: C, 71.82; H 3.72; N, 7.82.

Instrumentation. UV/Vis absorption spectra were measured on a JASCO V-570 spectrophotometer. Fluorescence spectra were measured on a JASCO FP-8600 fluorescence spectrophotometer. Absolute fluorescence quantum yields were determined by Hamamatsu Photonics C9920–01 Absolute PL Quantum Yield Measurement System. This instrument consisted of an integrating sphere equipped with a monochromatized Xe arc lamp as the light source and a multichannel spectrometer. The sensitivity of this system was fully calibrated for the spectral region 250-950 nm using deuterium and halogen standard light sources. A cylindrical quartz cuvette with 17 mm diameter for solid samples was set in the integrating sphere. Fluorescence lifetime measurements were made by using a laser diode (470 nm, pulse width ~500 ps, repetition

rate 20 kHz) as the excitation light source and a time-correlated single-photon counting fluorometer (Hamamatsu, Quantaurus-Tau C11367). The analysis of the fluorescence decay curves were carried out using the deconvolution method. Differential scanning calorimetry was performed on a METTLER TOLEDO DSC822e at heating and cooling rates of 10 °C min^{-1} under a nitrogen atmosphere. Powder X-ray diffraction measurements were performed on RIGAKU RINT-TTR III and carried out with Cu(Kα) radiation from an X-ray tube with a 0.5 × 10 mm^2 filament operated at 50 kV × 300 mA (15 kW).

Preparation of ground and fumed samples. Ground samples were prepared by using an agate mortar with a pestle. The stress (100-200 MPa) in the grinding treatment was measured by load cell and calculated according to Hertz contact theory.[1] The obtained ground sample was placed into a small glass vessel, which was placed into a large glass vessel containing various solvent (hexane, benzene, chloroform, acetone, acetonitrile, and methanol). Then, the large vessel was sealed with screw-cap for the saturation of solvent vapor and was allowed to stand for 1-2 hours to give fumed sample.

1 T. Ishi-i, H. Tanaka, R. Youfu, N. Aizawa, T. Yasuda, S.-i. Kato and T. Matsumoto, *New J. Chem*., 2019, **43**, 4998–5010.

2 L. Yao, Y. Pan, X. Tang, Q. Bai, F. Shen, F. Li, P. Lu, B. Yang and Y. Ma, *J. Phys. Chem. C*, 2015, **119**, 17800−17808.

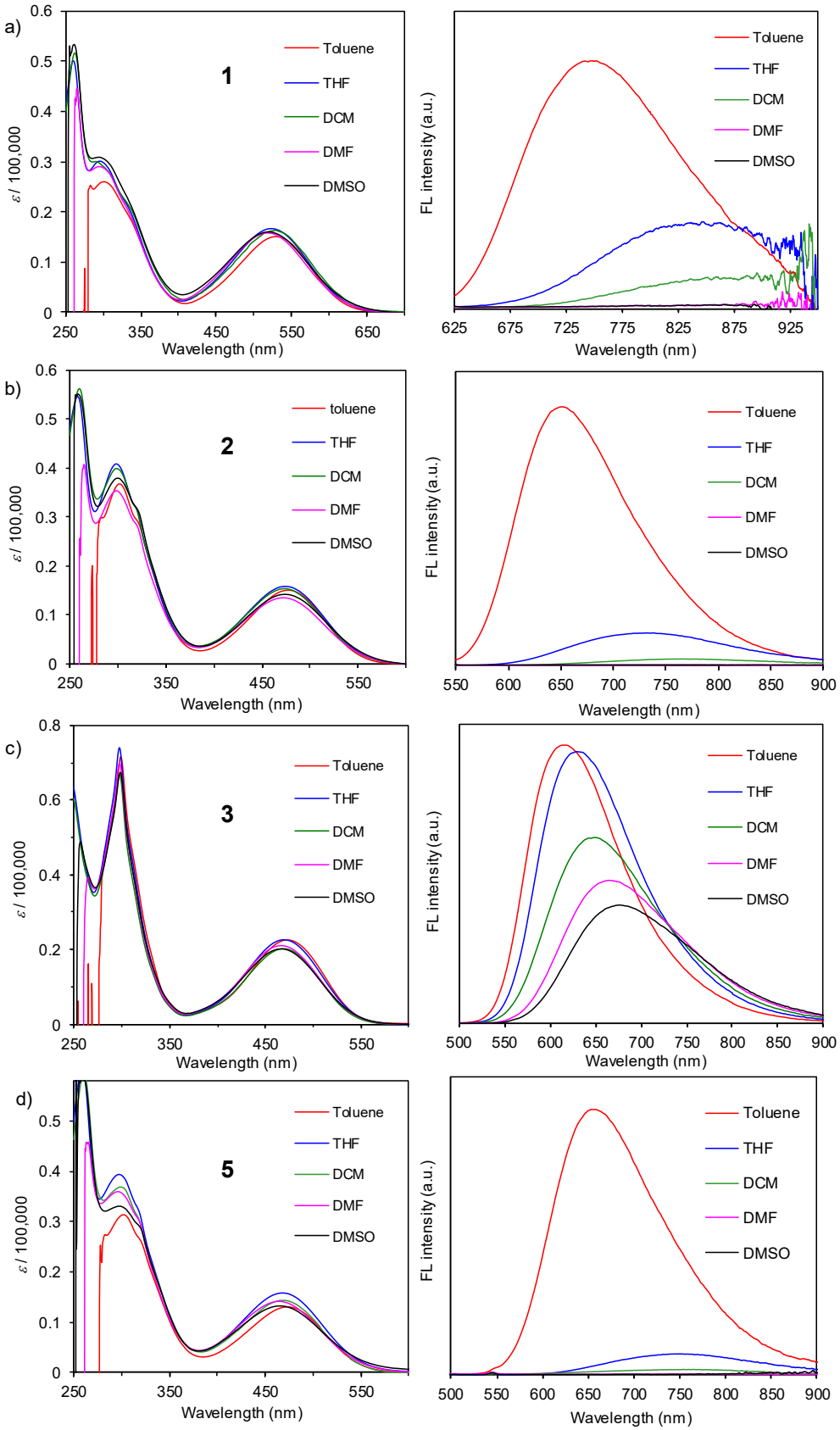

Fig. S1 UV/Vis absorption (left, 1.0×10^{-5} M) and fluorescence spectra (right, 1.0×10^{-6} M) of (a) **1**, (b) **2**, (c) **3**, and (d) **5** in toluene, THF, DCM, DMF, and DMSO.

Table S1 Spectral data of **1**, **2**, **3**, **4**, and **5** in solution

Comp.	Solvent	λ_{abs} (nm) [a]	ε	λ_{ex} (nm)	λ_{em} (nm) [b]	Φ_F [c]
1	Toluene	530	15,050	520	745	0.181
		301	25,980			
	THF	523	16,740	520	842	0.007
		296	30,120			
		260	50,060			
	DCM	529	16,310	520	875	0.002
		262	51,740			
	DMF	519	15,930	520	*d*	*d*
		295	29,150			
	DMSO	521	16,100	520	*d*	*d*
		294	53,460			
2	Toluene	479	15,160	470	652	0.501
		302	36,880			
	THF	475	15,880	470	738	0.080
		299	40,950			
		258	54,750			
	DCM	475	15,460	470	766	0.021
		299	40,030			
		260	56,340			
	DMF	473	13,510	470	*d*	*d*
		299	35,360			
	DMSO	474	14,200	470	*d*	*d*
		300	37,960			
		259	55,150			
3	Toluene	473	22,500	480	616	0.940
		300	71,500			
	THF	470	22,660	480	629	0.912
		298	74,050			
	DCM	470	20,330	480	649	0.720
		298	66,830			
	DMF	467	20,960	480	665	0.685
		298	69,780			
	DMSO	467	20,160	480	676	0.644
		299	67,400			
		257	48,840			
4 [e]	Toluene	507	25,150	500	646	0.40
	THF	504	24,450	500	665	0.20
	DCM	506	23,070	500	683	0.07
	DMF	501	23,400	500	*d*	*d*
5	Toluene	474	13,090	470	654	0.421
		302	31,340			
	THF	469	15,680	470	752	0.370
		298	36,230			
		259	60,430			
	DCM	468	14,270	470	765	0.129
		300	37,140			
		261	59,780			
	DMF	465	14,160	470	*d*	*d*
		296	35,950			
		265	45,750			
	DMSO	465	13,230	470	*d*	*d*
		297	33,060			
		260	58,700			

[a] at 1.0×10^{-5} M. [b] at 1.0×10^{-6} M. [c] Determined relative to fluorescein (Φ_{FL} 0.88, ex 460 nm) in NaOH aqueous solution. [d] Due to the low fluorescence intensity, the emission band could not be detected reliably. [e] Reported data: T. Ishi-i, K. Ikeda, M. Ogawa and Y. Kusakaki, *RSC Adv.*, 2015, **5**, 89171–89187.

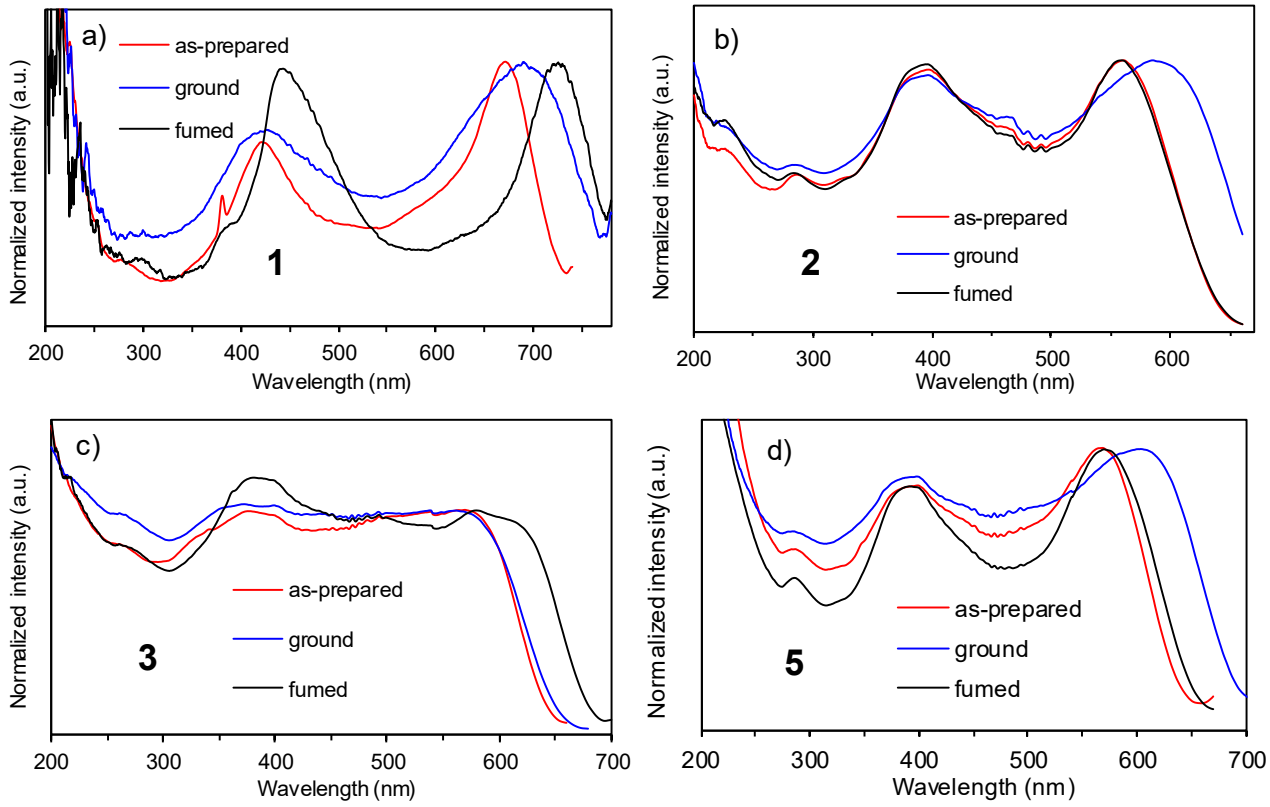

Fig. S2 Excitation spectra of (a) **1**, (b) **2**, (c) **3**, and (d) **5** in the as-prepared, ground, and fumed states: fumed solvent, chloroform, chloroform, dichloromethane, and chloroform for **1**, **2**, **3**, and **5**, respectively.

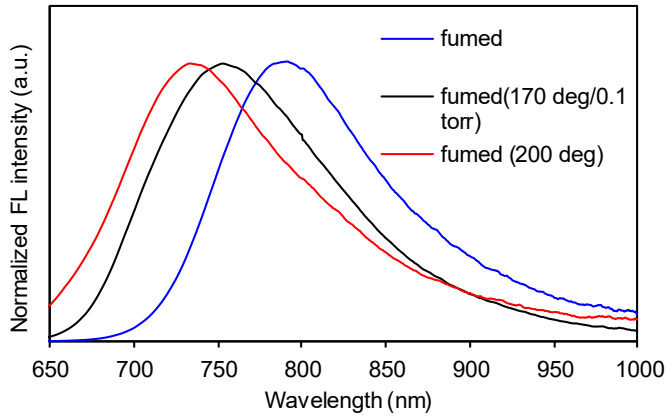

Fig. S3 Fluorescence spectra of **1** in the different solid state before and after heating (at 170 °C/0.1 torr and at 200 °C) of the chloroform-fuming sample.

The different fluorescence spectra observed in the heated state indicates the collapse of the porous crystal structure created in the fumed state.

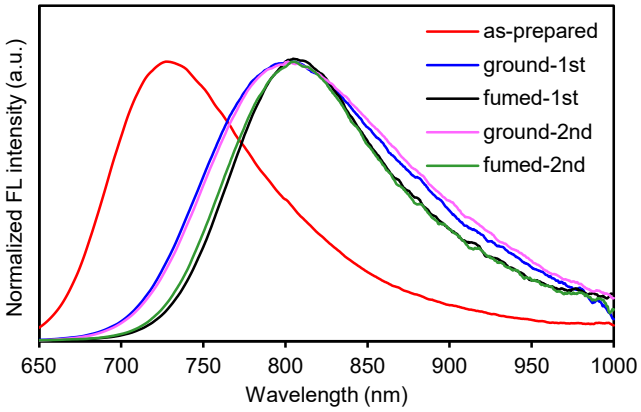

Fig. S4 Fluorescence spectra (ex, 440 nm) of **1** in the as-prepared, ground, and fumed (methanol) solid state: the grinding and fuming treatments were repeated twice.

In this methanol vapor-fuming system, the fluorescence switching between the ground state and fumed state was repeated reproducibly and reliably.

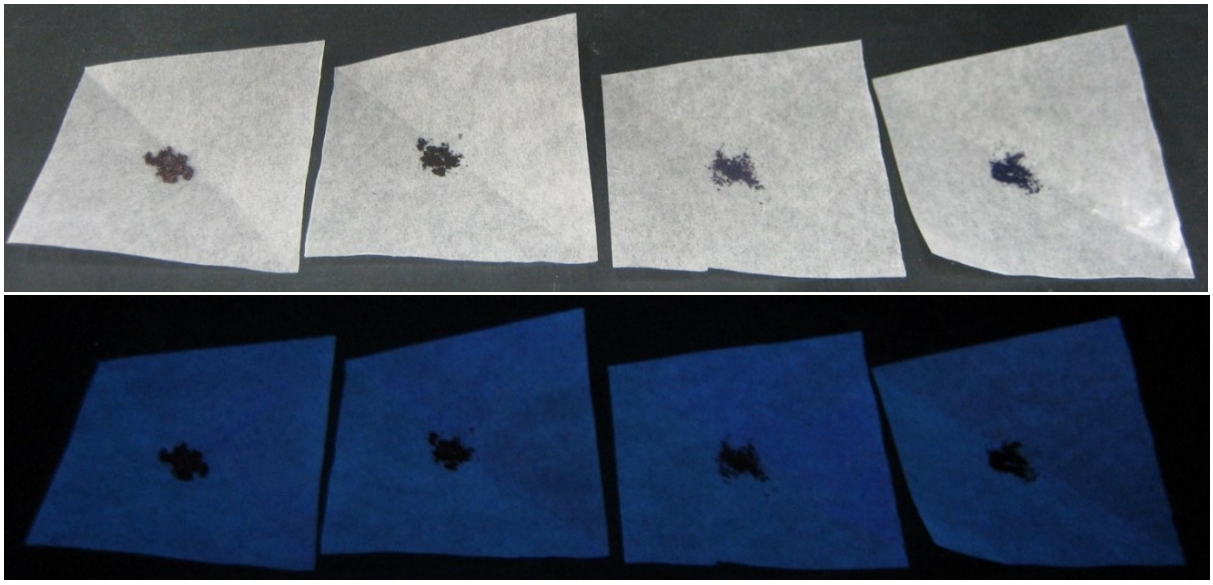

Fig. S5. Color (top) and fluorescence (bottom) images of **1** (as-prepared, ground, fumed (hexane), and fumed (methanol) state, from left to right) under the UV light irradiation. In the color images, the as-prepared sample indicates a brownish violet color, compared to the violet color in the ground, fumed (hexane), and fumed (methanol) state. In the fluorescence images, the near-infrared emission cannot be observed because of the out of visible region.

Table S2 Spectral data of **1**, **2**, **3**, **4**, and **5** in the solid state.

comp.	state	em (nm) [a]	λ_{ex} (nm)	ex (nm) [b]	λ_{em} (nm)	Φ_F (%) [c]
1	as-prepared	760	672	520	727	9.2
	ground	800	690	520	800	3.0
	fumed (chloroform)	800	726	520	792	2.6
	fumed (hexane)	800	699	520	776	4.4
	fumed (benzene)	800	713	520	789	3.3
	fumed (acetone)	800	726	520	794	2.5
	fumed (acetonitrile)	800	734	520	803	1.9
	fumed (methanol)	800	740	520	805	1.3
	fumed (chloroform) and heated (200 ℃)	760	671	520	733	3.4
	fumed (chloroform) and heated (170 ℃/0.1 torr)	780	664	520	753	8.4
2	as-prepared	690	561	470	656	38.0
	ground	690	584	470	695	25.0
	fumed (chloroform)	690	559	470	662	36.0
3	as-prepared	680	570	480	660	8.5
	ground	700	562	480	664	19.0
	fumed (dichloromethane)	720	580	480	677	10.5
4 [d]	as-prepared	680	593	520	655	58.0
	ground	680	617	520	692	37.0
	fumed (chloroform)	680	596	520	656	50.0
5	as-prepared	690	568	470	650	13.3
	ground	730	604	470	703	14.9
	fumed (chloroform)	690	570	470	669	20.3

[a] Monitored emission wavelength. [b] Excitation wavelength. [c] Absolute fluorescence quantum yield determined by an integrating sphere system. [d] Reported data: T. Ishi-i, H. Tanaka, R. Youfu, N. Aizawa, T. Yasuda, S.-i. Kato and T. Matsumoto, *New J. Chem*., 2019, **43**, 4998–5010.

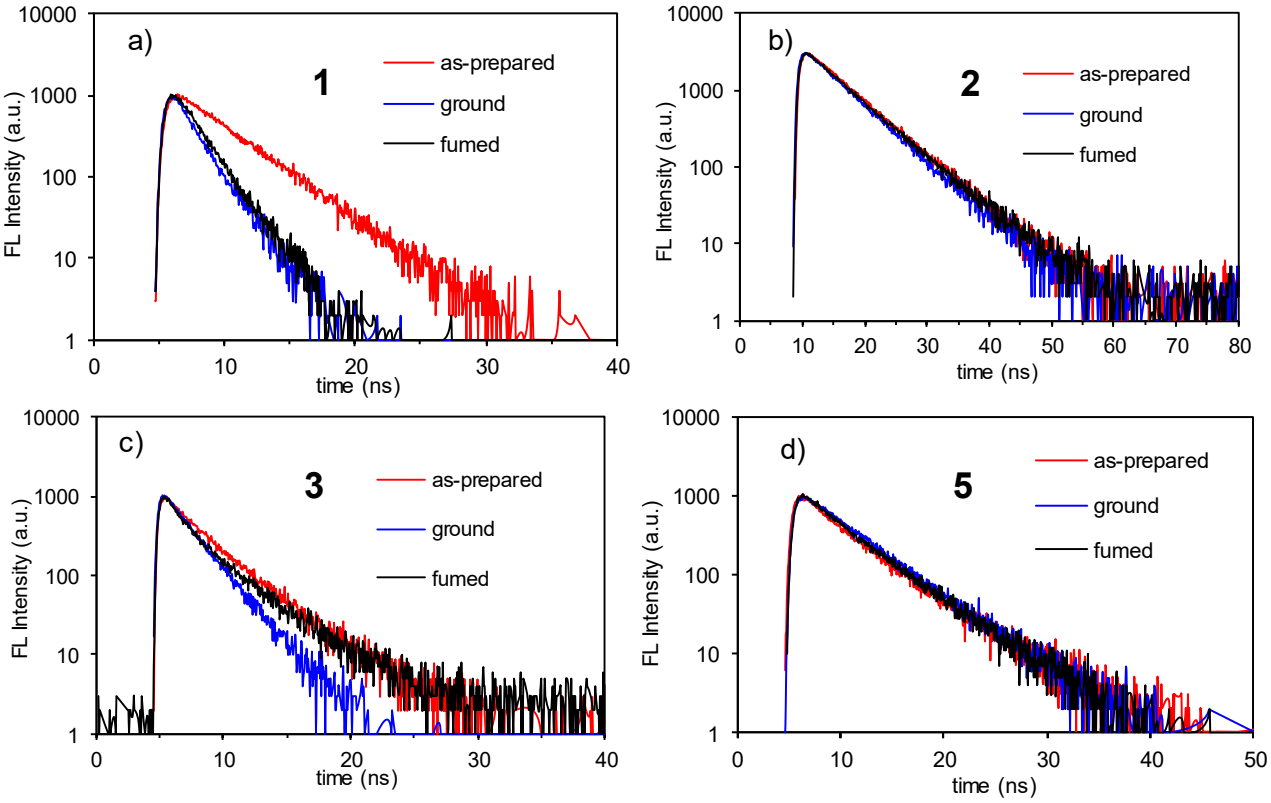

Fig. S6 Fluorescence decay curves of (a) **1**, (b) **2**, (c) **3**, and (d) **5** in the as-prepared, ground, and fumed (chloroform or dichloromethane) states monitored at fluorescence maxima with excitation at 470 nm.

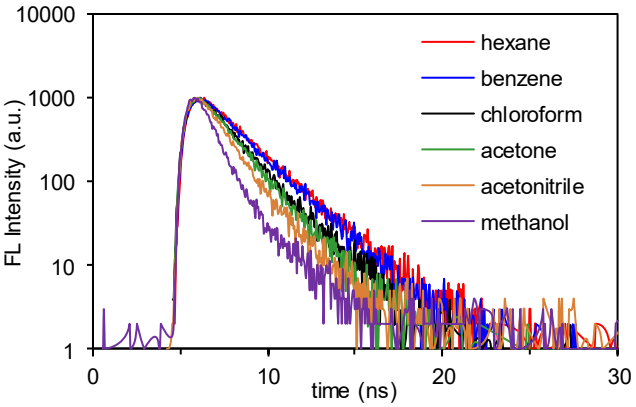

Fig. S7 Fluorescence decay curves of the fumed solid samples of **1** with different solvent vapors: hexane, benzene, chloroform, acetone, acetonitrile, and methanol.

Table S3 Fluorescence quantum yields, lifetime, and kinetic constants for **1**, **2**, **3**, **4**, and **5** in the solid state

comp.	state	Φ_f [%]	τ_f [ns] (f_i [%]) [a]	$<\tau_f>$ [ns] [b]	k_f [10^7 s^{-1}] [c]	k_{nr} [10^7 s^{-1}] [c]
1	as-prepared	9.2	3.63	-	2.5	25
	ground	3.0	1.43	-	2.1	68
	fumed (hexane)	4.4	1.99	-	2.2	48
	fumed (benzene)	3.3	1.95	-	1.7	50
	fumed (chloroform)	2.6	1.61	-	1.6	61
	fumed (acetone)	2.5	1.50	-	1.7	65
	fumed (acetonitrile)	1.9	1.22	-	1.6	80
	fumed (methanol)	1.3	0.79	-	1.7	130
2	as-prepared	38.0	6.05	-	6.3	10
	ground	25.0	5.61	-	4.5	13
	fumed (chloroform)	36.0	4.83 (43) 6.89 (57)	6.18	5.8	10
3	as-prepared	8.5	3.01 (24) 6.78 (76)	6.31	1.4	15
	ground	19.0	3.01 (38) 4.63 (62)	4.16	4.6	20
	fumed (dichloromethane)	10.5	2.62 (44) 7.62 (56)	9.40	1.1	9.5
4 [d]	as-prepared	58.0	6.54	-	8.9	6.4
	ground	37.0	4.34	-	8.5	15
	fumed (chloroform)	50.0	5.61	-	8.9	8.9
5	as-prepared	13.3	2.11 (32) 5.16 (68)	4.67	2.8	19
	ground	14.9	3.02 (16) 4.70 (84)	4.51	3.3	19
	fumed (chloroform)	20.3	2.11 (20) 4.78 (80)	4.52	4.4	18

[a] The value in parentheses is the fractional contribution of component i to the total steady-state intensity, which was calculated by $f_i = (A_i\tau_{fi}/\Sigma A_i\tau_{fi})\times 100$. [b] The intensity-averaged decay lifetime ($<\tau>$) was calculated as follows: $<\tau> = \Sigma(A_n\tau_n^2)/\Sigma(A_n\tau_n)$, in which A_n is the coefficient of each exponential term. [c] Fluorescence radiative rate constant (k_f) and nonradiative rate constant (k_{nr}) were calculated as follows: $\Phi_{FL} = k_f/(k_f + k_{nr}) = k_f<\tau>$, $<\tau> = 1/(k_f + k_{nr})$. [d] Reported data: T. Ishi-i, H. Tanaka, R. Youfu, N. Aizawa, T. Yasuda, S.-i. Kato and T. Matsumoto, *New J. Chem*., 2019, **43**, 4998–5010.

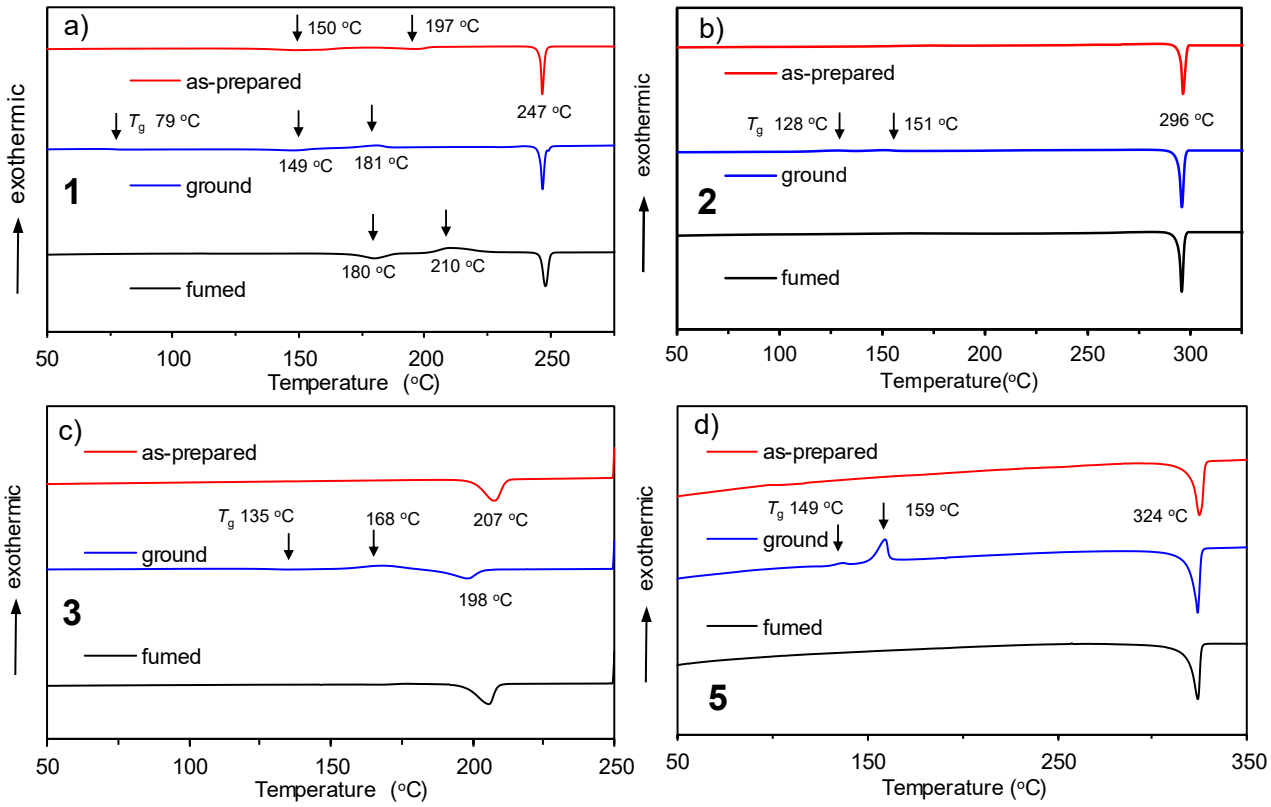

Fig. S8 DSC curves of (a) **1**, (b) **2**, (c) **3**, and (d) **5** in the as-prepared, ground, and fumed state: fumed solvent, chloroform, chloroform, dichloromethane, and chloroform for **1**, **2**, **3**, and **5**, respectively.

In the three samples of **1**, weak peaks (at 150 and 197 °C for as-prepared sample, at 149 and 181 °C for ground sampl, and at 180 and 210 °C for fumed sample) were observed in addition to the melting point (247 °C). Probably, phase transion was performed at the temparature. Finally, same solid state was gived at the higher temperatre in the three samples, judging from the same melting point.

All the ground samples provide the glass transition temperature (T_g) (79 °C for **1**, 128 °C for **2**, 135 °C for **3**, and 149 °C for **5**), indicating the formation of minimally ordered amorphous-like state.

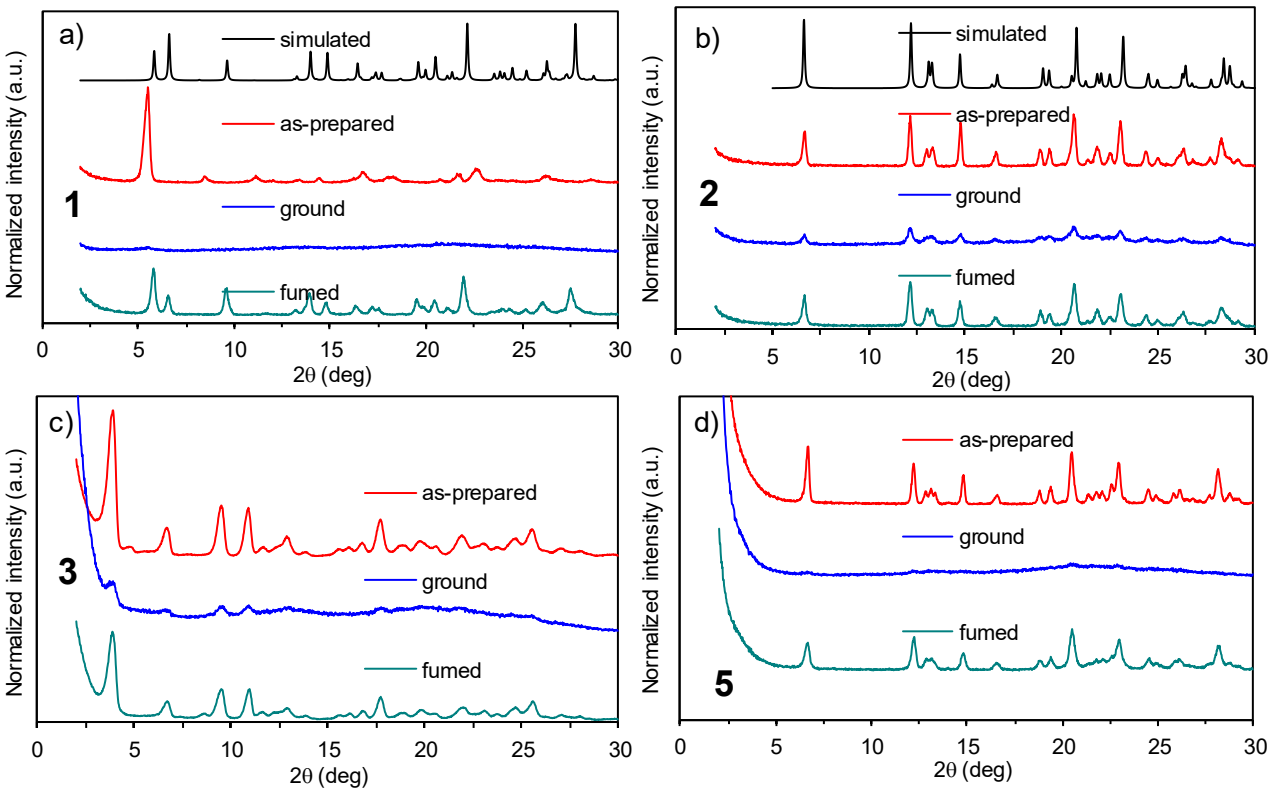

Fig. S9 Powder XRD patterns of (a) **1**, (b) **2**, (c) **3**, and (d) **5** in the as-prepared, ground, and fumed state and the simulated powder patterns of the fumed sample in **1** and of the as-prepared sample in **2** derived from a single crystal: fumed solvent, chloroform, chloroform, dichloromethane, and chloroform for **1**, **2**, **3**, and **5**, respectively.

All the ground samples provide the weak and broadened reflections, indicating the formation of minimally ordered amorphous-like state.

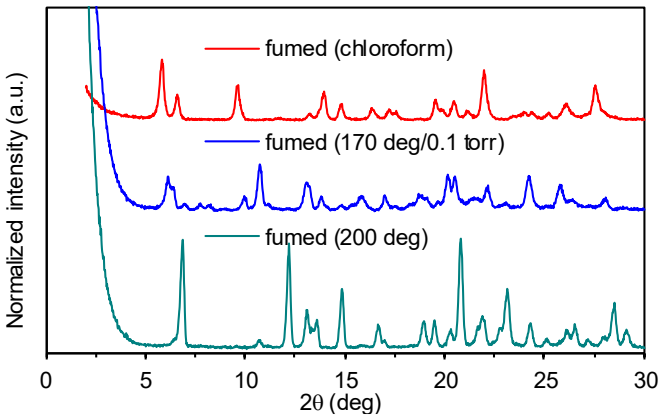

Fig. S10 Powder XRD patterns **1** in the different solid state before and after heating (at 170 °C/0.1 torr and at 200 °C) of the chloroform-fuming sample.

The different XRD pattern observed in the heated state indicates the collapse of the porous crystal structure created in the fumed state.

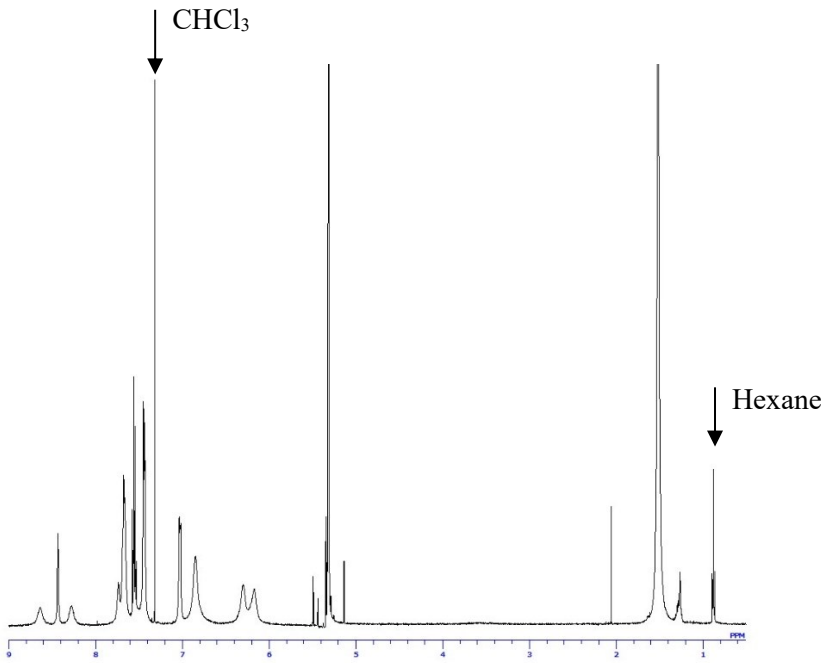

Fig. S11 ^{1}H NMR spectrum of the as-prepared solid sample of **1** in CD_2Cl_2, which indicates the remaining chloroform (7.32 ppm) and hexane (0.85, 1.25 ppm). The molar ratio of **1**:chloroform:hexane was confirmed by integration to be 1:0.64:0.14 (mol/mol/mol).

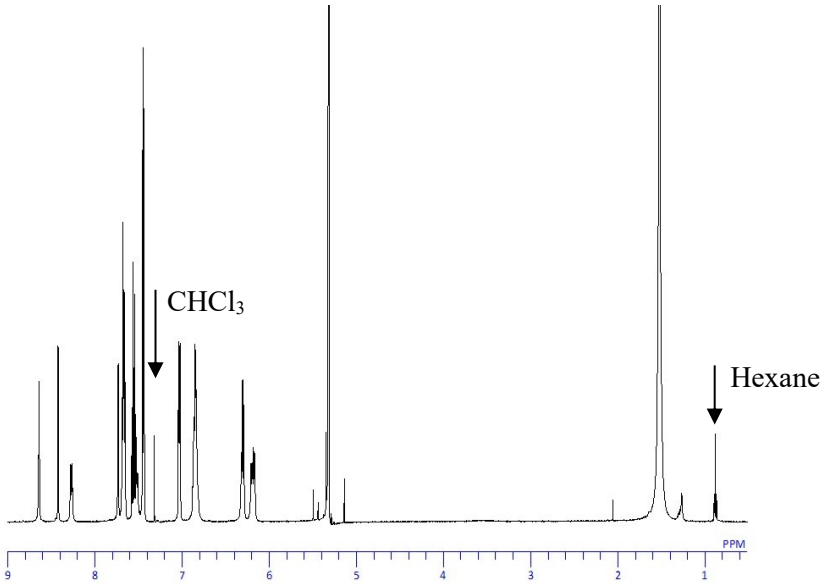

Fig. S12 ^{1}H NMR spectrum of the ground solid sample of **1** in CD_2Cl_2, which indicates the remaining chloroform (7.32 ppm) and hexane (0.85, 1.25 ppm). The molar ratio of **1**:chloroform:hexane was confirmed by integration to be 1:0.13:0.06 (mol/mol/mol). The obtained molar ratio indicated that a portion of included chloroform and hexane molecules released after mechanical grinding.

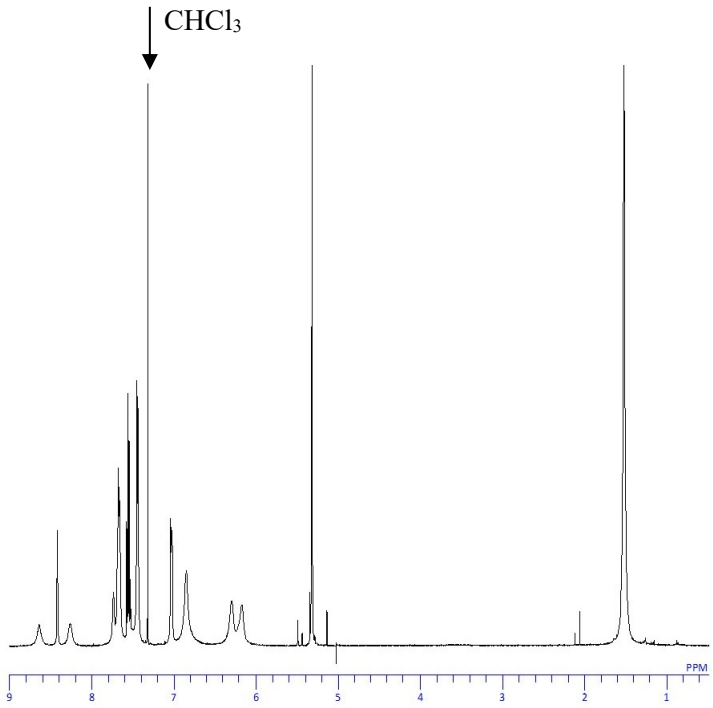

Fig. S13 ^{1}H NMR spectrum of the fumed (chloroform) solid sample of **1** in CD_2Cl_2, which indicates the remaining chloroform (7.32 ppm). The molar ratio of **1**:chloroform was confirmed by integration to be 1:0.80 (mol/mol).

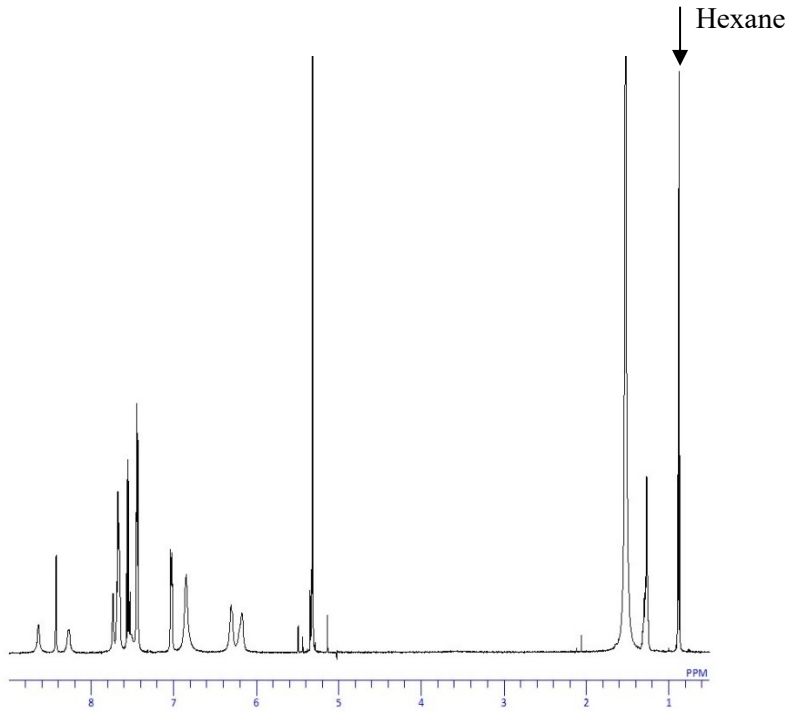

Fig. S14 ^{1}H NMR spectrum of the fumed (hexane) solid sample of **1** in CD_2Cl_2, which indicates the remaining hexane (0.85, 1.25 ppm). The molar ratio of **1**:hexane was confirmed by integration to be 1:0.52 (mol/mol). The obtained molar ratio indicated that all the included chloroform molecules were exchanged to hexane molecules used as fuming solvent.

Table S4 The remaining solvent molecules used as fuming solvent for **1** confirmed by ^{1}H NMR integration.

state	**1**:solvent (mol/mol)
as-prepared [a]	**1**:chloroform:hexane (1:0.64:0.14)
ground	**1**:chloroform:hexane (1:0.13:0.06)
fumed (chloroform)	**1**:chloroform (1:0.80)
fumed (hexane)	**1**:hexane (1:0.52)
fumed (benzene)	**1**:benzene (1:0.25)
fumed (acetone)	**1**:acetone (1:0.16)
fumed (acetonitrile)	**1**:acetonitrile (1:0.15)
fumed (methanol)	**1**:methanol (1:0.23)
fumed (chloroform) and heated (200 °C)	**1**:chloroform (1:<0.01)
fumed (chloroform) and heated (170 °C/0.1 torr)	**1**:chloroform (1:<0.01)

[a] The as-prepared sample was obtained by recrystallization from chloroform/hexane.

Single crystal X-ray diffraction analysis

The single crystals for the X-ray diffraction analysis in **1** and **2** were obtained by the slow diffusion of hexane into the chloroform solution of dyes. All measurements were made on a Rigaku Saturn724 diffractometer using multi-layer mirror monochromated Mo-Kα radiation. The structure was solved by direct methods[1] and expanded using Fourier techniques. The non-hydrogen atoms were refined anisotropically. Hydrogen atoms were refined using the riding model. All calculations were performed using the CrystalStructure[2] crystallographic software package except for refinement, which was performed using SHELXL2013.[3] Simulated powder patterns were generated with Mercury 4.0 from the structures determined by single crystal diffraction analyses. The crystal structure of **1** contained disordered solvent molecules, which were used in the recrystallization. Thus, the crystal structure was refined by using PLATON SQUEEZE program.

1 M. C. Burla, R. Caliandro, M. Camalli, B. Carrozzini, G. L. Cascarano, L. De Caro, C. Giacovazzo, G. Polidori, D. Siliqi and R. Spagna, *J. Appl. Cryst*., 2007, **40**, 609–613.

2 Crystal Structure Analysis Package, Rigaku Corporation (2000-2014). Tokyo 196-8666, Japan.

3 G. M. Sheldrick, *Acta Cryst*., 2008, **A64**, 112–122.

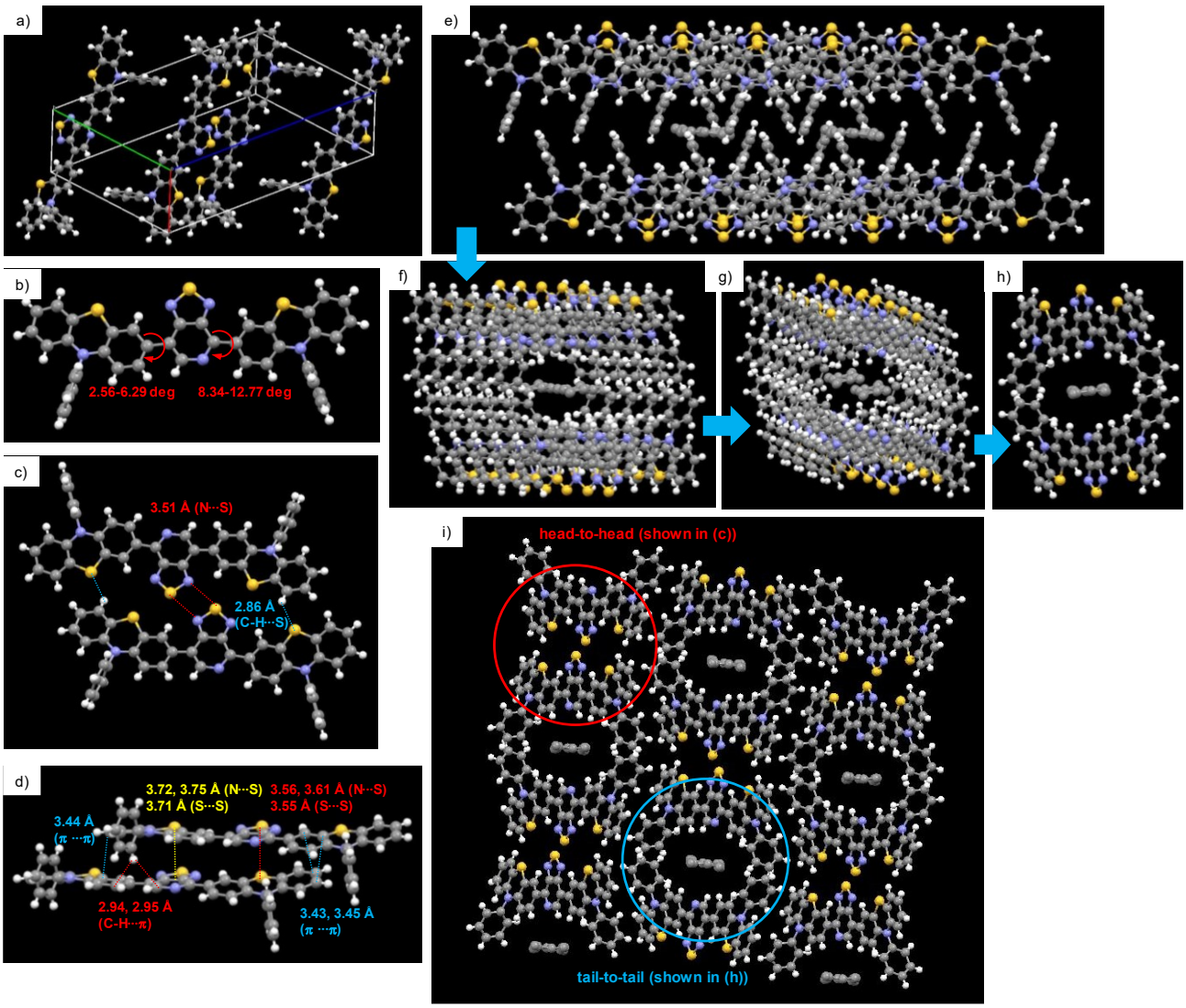

Fig. S15 Crystal structure of **1**: (a) unit cell packing, (b) monomeric structure with planar conformation, (c) parallel dimeric structure (head-to-head arrangement for thiadiazolopyridine moieties), (d) perpendicular dimeric structure bearing tight packing, (e)-(h) packing structure of a set of perpendicularly stacked pentamer with different view angle (tail-to-tail arrangement for thiadiazolopyridine moieties), and (i) two-dimensional packing composed of head-to-head and tail-to-tail arrangement shown in Figs. S15c and S15h.

In this crystal packing structure, intermolecular short contacts between hydrogen atom and sulfur atom and between nitrogen atom and sulfur atom were found in a parallel dimeric structure (Fig. S15c). These C-H···S and S···N interactions[1] cooperatively work to stabilize the crystal structure, in addition to other noncovalent interactions.

1 K. Hayashi, S. Ogawa, S. Sano, M. Shiro, K. Yamaguchi, Y. Sei and Y. Nagao, *Chem. Pharm. Bull.*, 2008, **56**, 802–806; M. Iwaoka, S. Takemoto, M. Okada and S. Tomoda, *Bull. Chem. Soc. Jpn.*, 2002, **75,** 1611–1625.

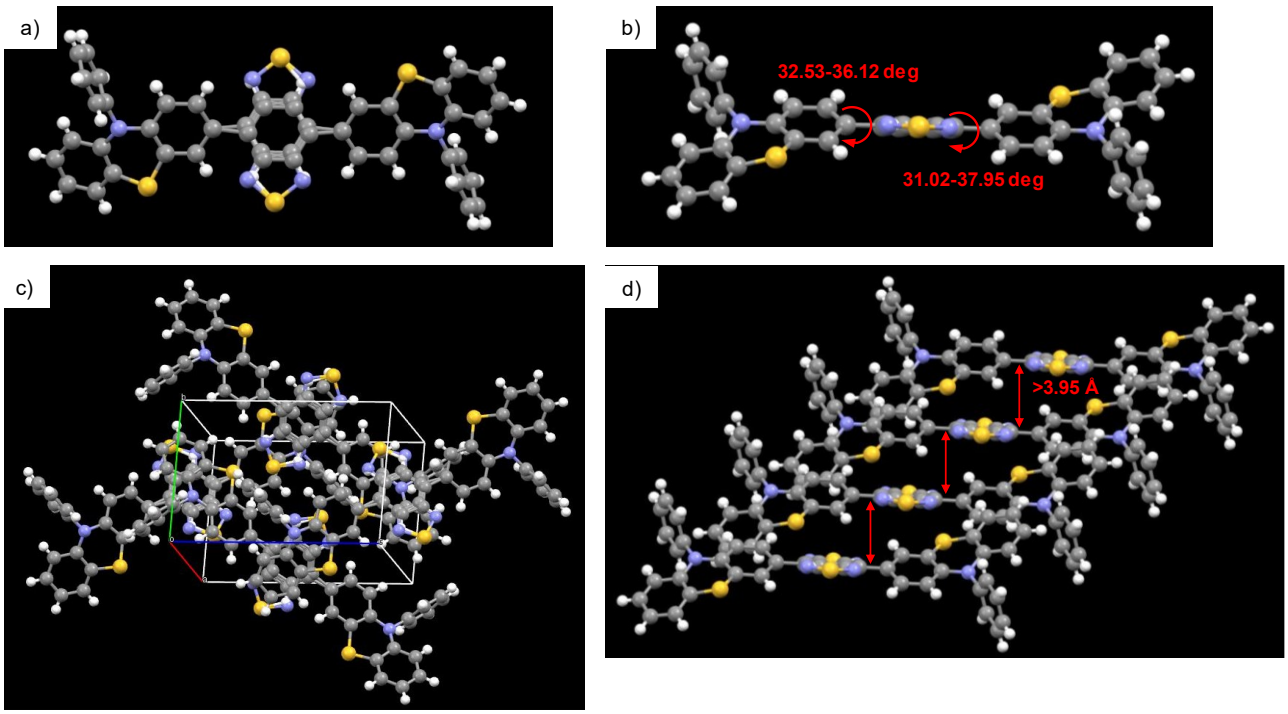

Fig. S16 Crystal structure of **2**: (a) top view and (b) side view of monomeric structure with twisted conformation, (c) unit cell packing, and (d) one-dimensional packing.

A static disorder structure was found in benzothiadiazole moiety, indicating chemically equivalent two orientations with a 50:50 probability.

In the one-dimensional packing, the benzothiadiazole core moieties are separated by a long distance of more than 3.95 Å, producing a space inside the one-dimensional structure. This loose packing allows rearrangement of the packing structure upon application of mechanical grinding, together with the assistance from the twisted structure, leading to mechanochromic fluorescence.

Table S5 Crystallographic data for **1** and **2**.

	1 (chloroform/hexane)	**2** (chloroform/hexane)
CCDC number	2012532	2012533
diffractometer	Saturn 724	Saturn 724
formula	$C_{41}H_{25}N_5S_3$	$C_{42}H_{26}N_4S_3$
M	683.86	682.87
T (K)	124	123.2
crystal system	monoclinic	monoclinic
space group	$P2_1/c$ (no. 14)	$P2_1/c$ (no. 14)
a (Å)	6.8794 (9)	13.843 (5)
b (Å)	18.315 (2)	8.651 (3)
c (Å)	26.670 (4)	13.883 (5)
α (°)		
β (°)	92.965 (3)	105.849 (10)
γ (°)		
V (Å^3)	3355.8 (8)	1599.4 (9)
Z	4	2
ρ_{calcd} (g cm^{-3})	1.353	1.418
μ (cm^{-1})	2.599 (MoKα)	2.717 (MoKα)
F (000)	1416	708
crystal size (mm^3)	0.14 × 0.05 × 0.01	0.20 × 0.10 × 0.01
reflections collected	32224	14856
reflections unique	7674	3638
R_{int}	0.0645	0.0658
data [$F^2 > 2\sigma(F^2)$]	6338	3638
parameters	442	208
goodness-of-fit	1.198	1.237
$R1/wR^2$ [$F^2 > 2\sigma(F^2)$]	0.0826/0.1676	0.1382/0.2844
$R1/wR^2$ (all data)	0.1001/0.1762	0.1705/0.3054
Max Shift/error in final cycle	0.001	0.000

Table S6 Atomic displacement parameters (U_{iso}) for **1** and **2**.

1				**2**	
atom	U_{iso}	atom	U_{iso}	atom	U_{iso}
S1	0.0370(2)	H23	0.042	S1	0.0488(7)
S2	0.0350(2)	C24	0.0284(6)	S2	0.0658(6)
S3	0.0396(2)	C25	0.0298(7)	N1	0.044(2)
N1	0.0322(6)	H25	0.036	N2	0.043(2)
N2	0.0315(6)	C26	0.0272(6)	N3	0.0532(13)
N3	0.0550(9)	C27	0.0291(7)	C1	0.03
N4	0.0310(6)	C28	0.0361(8)	C2	0.036
N5	0.0325(6)	H28	0.043	C3	0.036
C1	0.0273(6)	C29	0.0402(8)	C4	0.044
C2	0.0281(6)	H29	0.048	H4	0.053
C3	0.0288(7)	C30	0.0395(8)	C5	0.043
C4	0.0388(8)	H30	0.047	H5	0.052
H4	0.047	C31	0.0355(7)	C6	0.035
C5	0.0309(7)	H31	0.043	C7	0.0509(14)
C6	0.0261(6)	C32	0.0301(7)	C8	0.0524(15)
C7	0.0287(6)	C33	0.0294(7)	H8	0.063
H7	0.034	C34	0.0343(7)	C9	0.0527(15)
C8	0.0264(6)	H34	0.041	C10	0.0500(14)
C9	0.0290(7)	C35	0.0309(7)	C11	0.0571(16)
C10	0.0318(7)	H35	0.037	H11	0.068
H10	0.038	C36	0.0312(7)	C12	0.0578(16)
C11	0.0332(7)	C37	0.0367(8)	H12	0.069
H11	0.04	H37	0.044	C13	0.0478(14)
C12	0.0328(7)	C38	0.0437(9)	C14	0.0473(14)
H12	0.039	H38	0.052	C15	0.0495(14)
C13	0.0317(7)	C39	0.0465(9)	H15	0.059
H13	0.038	H39	0.056	C16	0.0570(16)
C14	0.0280(6)	C40	0.0490(10)	H16	0.068
C15	0.0279(6)	H40	0.059	C17	0.0513(15)
C16	0.0337(7)	C41	0.0418(8)	H17	0.062
H16	0.04	H41	0.05	C18	0.0510(14)
C17	0.0321(7)			H18	0.061
H17	0.039			C19	0.0527(15)
C18	0.0291(7)			C20	0.0603(17)
C19	0.0385(8)			H20	0.072
H19	0.046			C21	0.0688(19)
C20	0.0427(8)			H21	0.083
H20	0.051			C22	0.074(2)
C21	0.0425(9)			H22	0.089
H21	0.051			C23	0.0615(17)
C22	0.0405(8)			H23	0.074
H22	0.049			C24	0.0640(18)
C23	0.0347(7)			H24	0.077

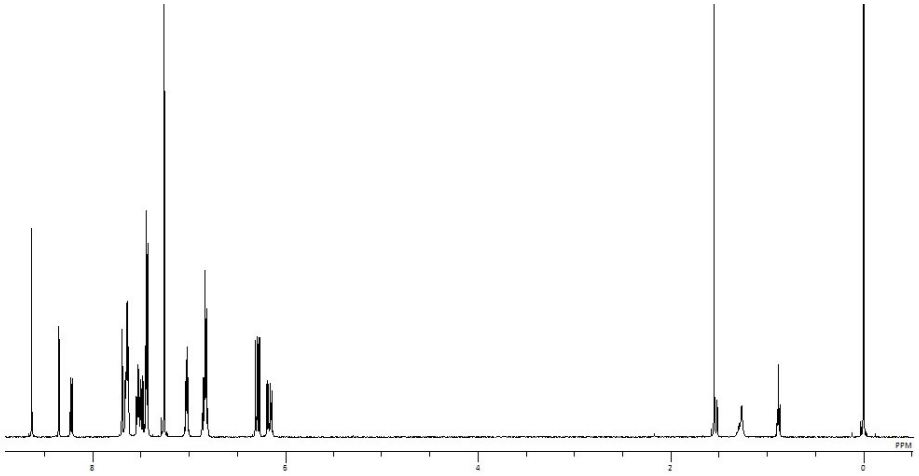

Fig. S17 ^{1}H NMR spectrum of **1** in $CDCl_3$.

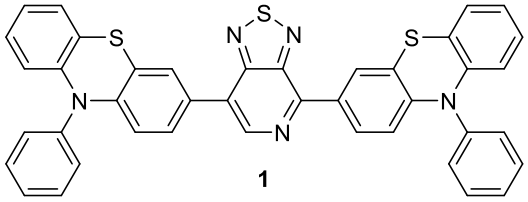

1

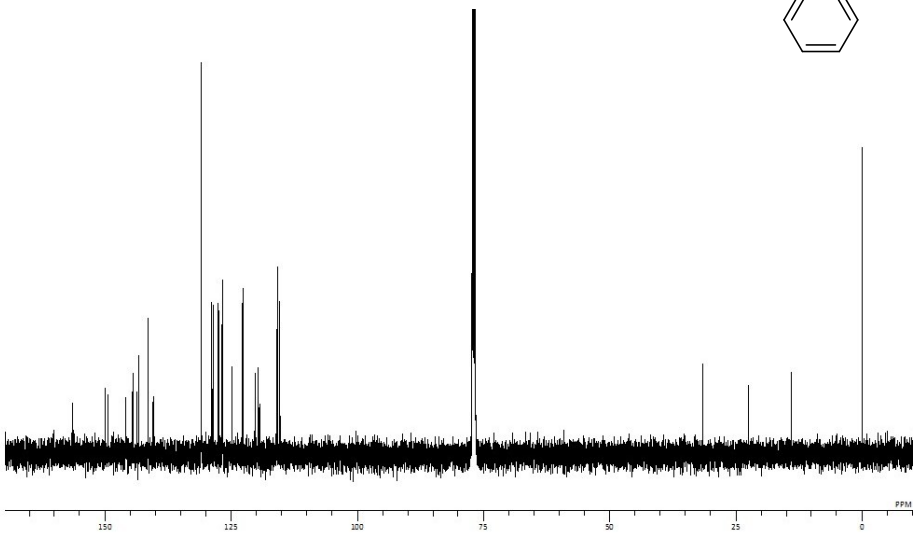

Fig. S18 ^{13}C NMR spectrum of **1** in $CDCl_3$.

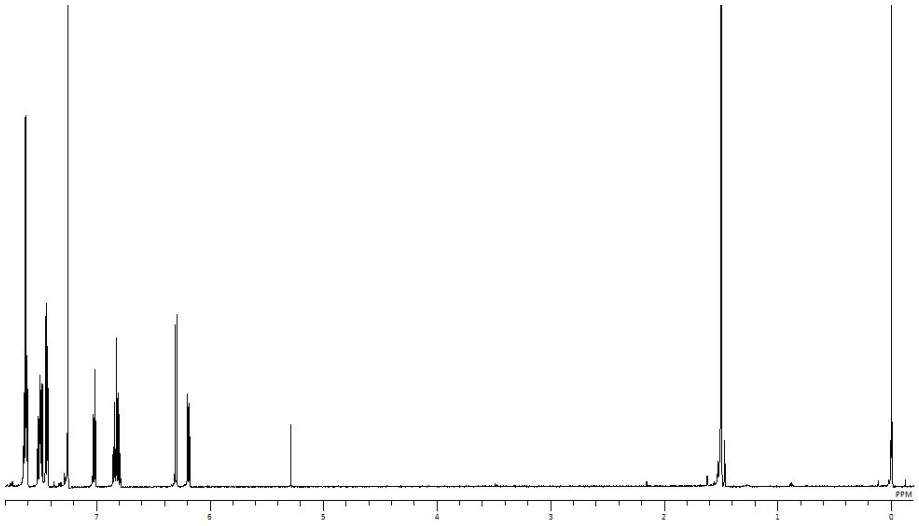

Fig. S19 ^{1}H NMR spectrum of **2** in $CDCl_3$.

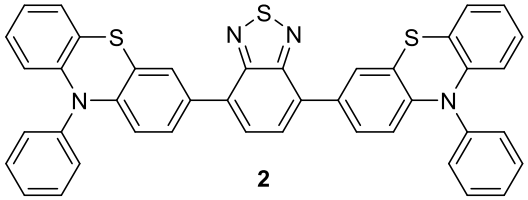

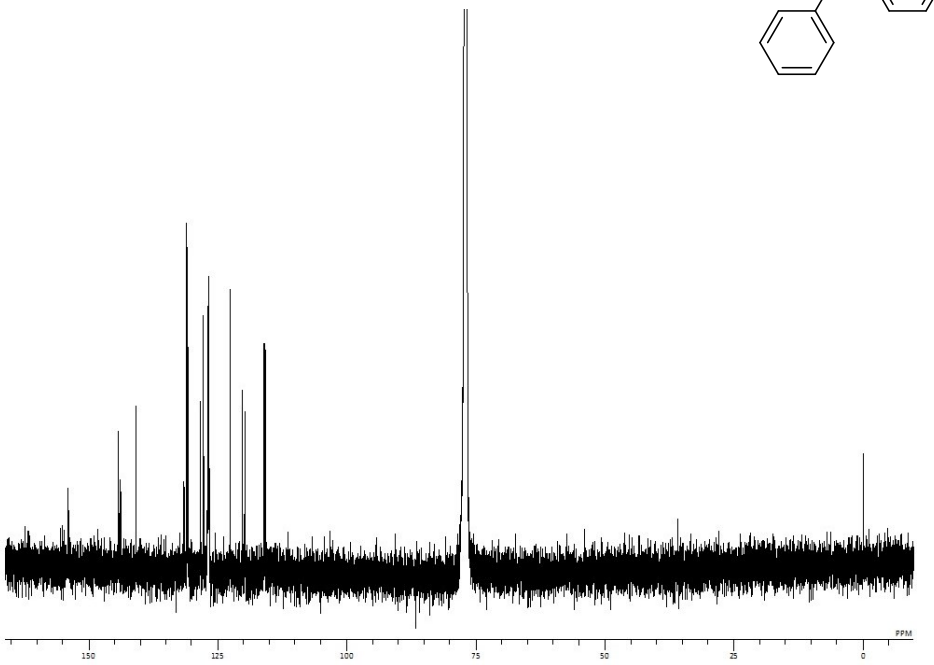

Fig. S20 ^{13}C NMR spectrum of **2** in $CDCl_3$.

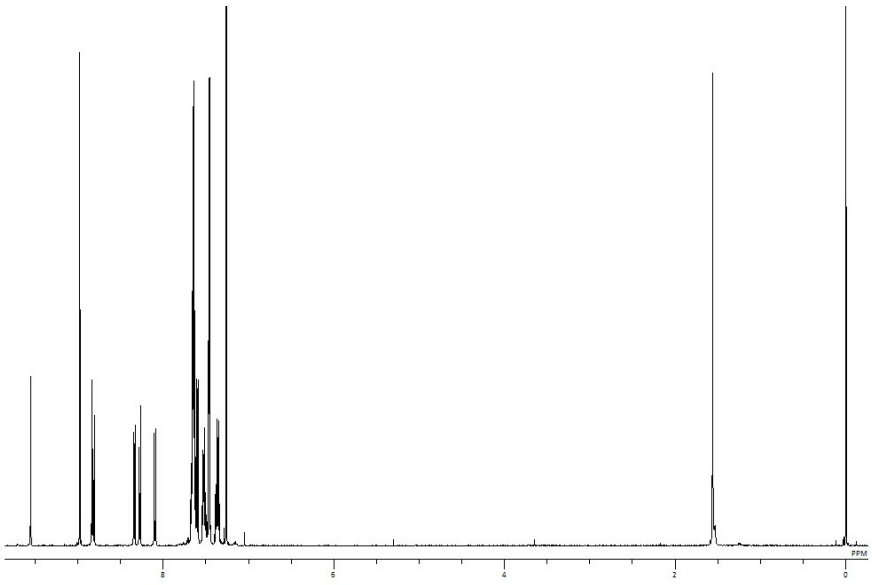

Fig. S21 ^{1}H NMR spectrum of **3** in $CDCl_3$.

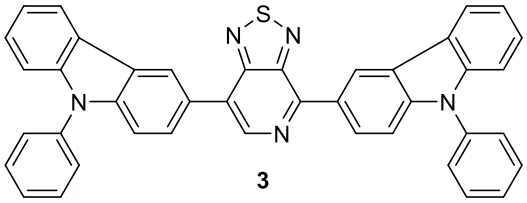

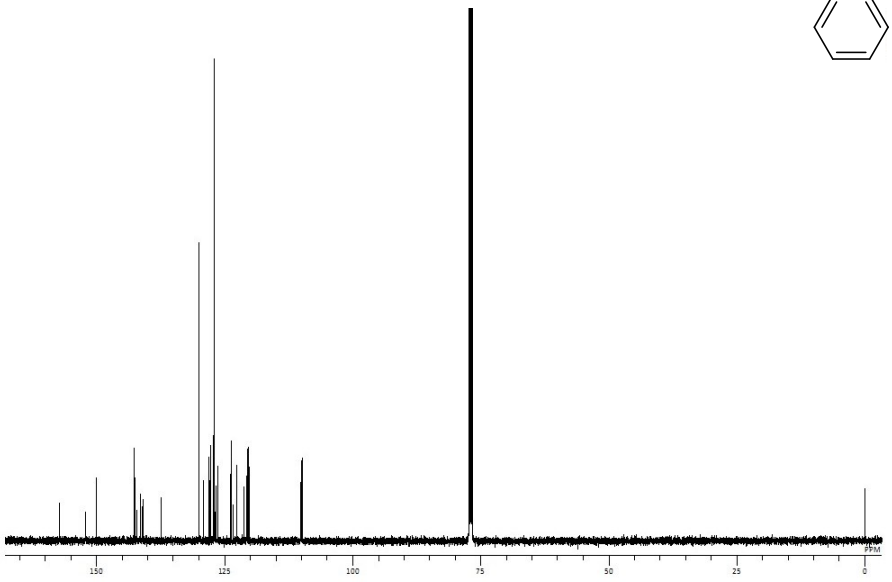

Fig. S22 ^{13}C NMR spectrum of **3** in $CDCl_3$.

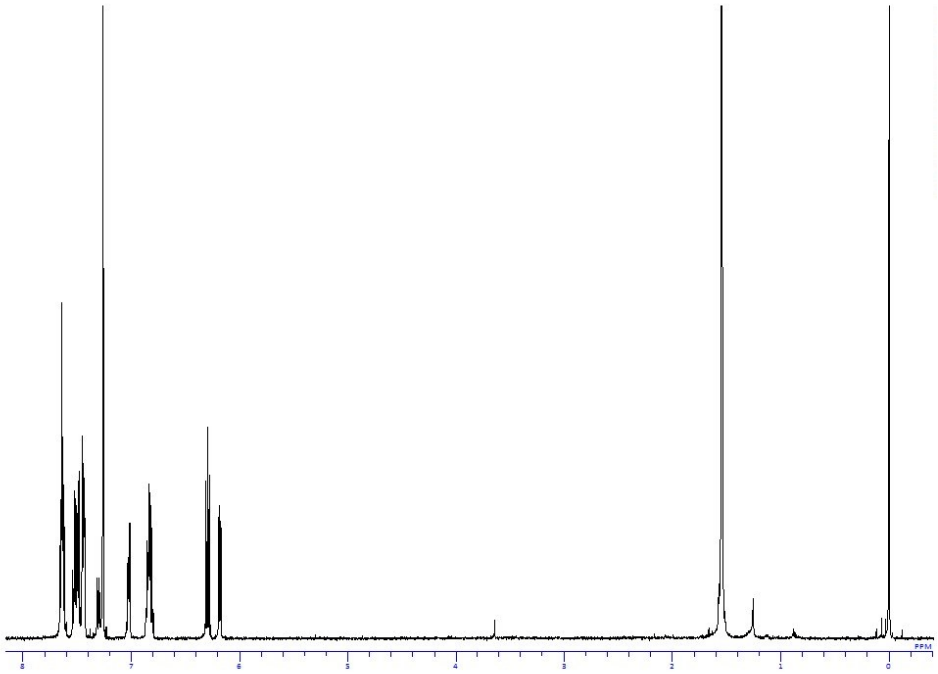

Fig. S23 ^{1}H NMR spectrum of **5** in $CDCl_3$.

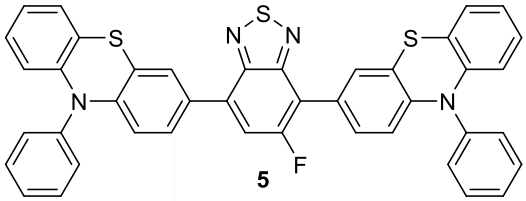

5

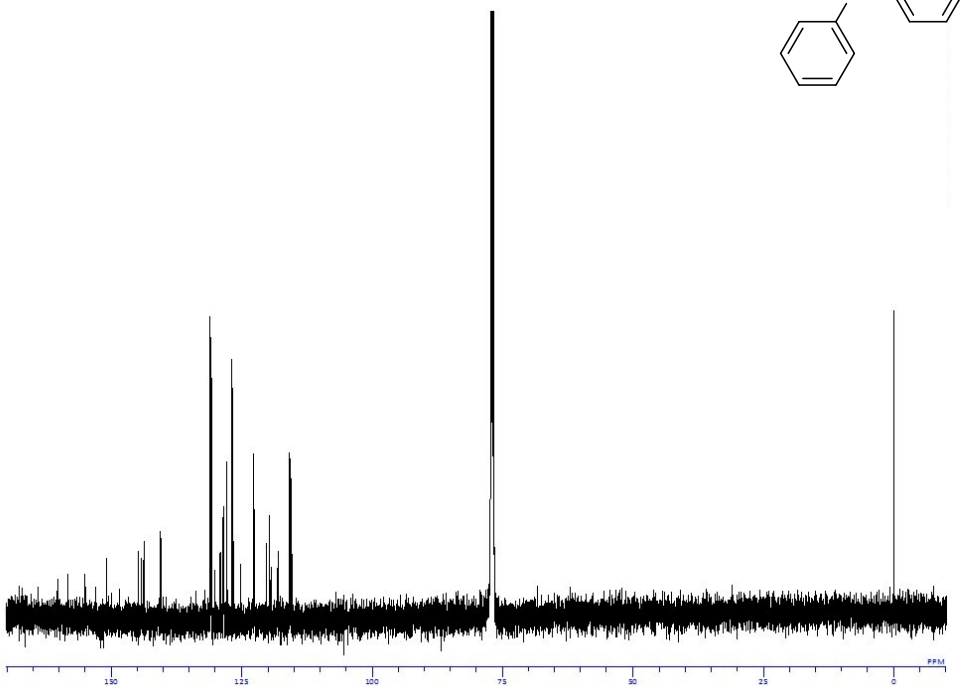

Fig. S24 ^{13}C NMR spectrum of **5** in $CDCl_3$.